Chemical Engineering Science 64 (2009) 4707 – 4718

Contents lists available at ScienceDirect

Chemical Engineering Science

journal homepage: www.elsevier.com/locate/ces

Relation between structure and gas transport properties of polyethylene oxide networks based on crosslinked bisphenol A ethoxylate diacrylate

Jeffrey J. Richards[a], Michael K. Danquah[a], Sumod Kalakkunnath[a], Douglass S. Kalika[a,*], Victor A. Kusuma[b], Scott T. Matteucci[b], Benny D. Freeman[b]

[a]Department of Chemical and Materials Engineering and Center for Manufacturing, University of Kentucky, Lexington, KY 40506-0046, USA
[b]Center for Energy and Environmental Resources, Department of Chemical Engineering, University of Texas at Austin, Austin, TX 78758, USA

ARTICLE INFO

Article history:
Received 29 August 2008
Accepted 24 November 2008
Available online 25 December 2008

Keywords:
Membranes
Polymers
Gases
Separations
Carbon dioxide
Thermal analysis

ABSTRACT

Poly(ethylene oxide) (PEO) networks prepared from the photopolymerization of bisphenol A ethoxylate diacrylate (BPA–EDA) have been investigated as a function of crosslinker molecular weight and copolymer composition. Dynamic mechanical and dielectric methods have been used to elucidate the thermal relaxation characteristics of the polymers as a function of network composition and architecture, and these properties were related to measured gas transport for CO_2 separations. Copolymerization strategies involving the insertion of flexible PEG side chains along the network backbone proved effective in enhancing network free volume and increasing permeability. The gas transport performance of rubbery amorphous membranes based on the $n = 15$ BPA–EDA crosslinker (i.e., crosslinker encompassing 30 ethylene oxide repeat units between crosslinks) compared favorably to model polymers synthesized from poly(ethylene glycol) diacrylate.

1. Introduction

The separation of acid gases such as carbon dioxide or hydrogen sulfide from mixtures with light gases is a process of considerable industrial importance and a number of mature technologies have been utilized to achieve such separations in a variety of applications; e.g., natural gas sweetening, or purification of hydrogen produced by steam reforming of hydrocarbons. The implementation of membrane technology for CO_2 separations offers significant advantages over more traditional approaches, given the benefits of membrane processes with respect to energy requirements, maintenance and physical footprint (Baker, 2004). For many such applications (e.g., CO_2/CH_4, CO_2/H_2 separations), highly permeable CO_2-selective membranes are required whereby CO_2 is preferentially permeated to the low-pressure side of the membrane while the light gas product stream is retained at or near the feed pressure (Lin et al., 2006c,d). Recently, poly(ethylene oxide) (PEO) has been identified as a promising gas separation membrane material for the selective removal of CO_2 (Lin and Freeman, 2004). The presence of polar ether oxygens leads to dispersive interactions with the quadrupole moment of CO_2 and favorable solubility selectivity for permeation of CO_2 over light gases (Lin and Freeman, 2005a).

The permeability of PEO polymer to acid gas molecules such as CO_2, and its corresponding viability as a gas separation membrane material, is limited by its strong tendency to crystallize (Lin and Freeman, 2004). However, it has been demonstrated that crystallization of PEO is suppressed in chemically crosslinked networks where the length of the ethylene oxide (EO) segments between crosslink junctions is limited to approximately 20 repeat units or less (Graham, 1987; Priola et al., 1993). Such networks can be prepared by the ultraviolet (UV) photopolymerization of poly(ethylene glycol) diacrylate (PEGDA), for example, where the effective distance between crosslinks is controlled by the molecular weight of the difunctional PEG monomer. This synthetic approach results in wholly-amorphous, rubbery polymers with high permeability and high CO_2 selectivity. Given the potential of these materials for use as gas separation membranes, we have explored a number of copolymerization strategies designed to modify the molecular architecture and chemical constitution of the networks in an effort to optimize their gas transport characteristics. These activities have resulted in the identification of model polymer systems with desirable gas separation properties. By combination of detailed thermal analysis studies (Borns et al., 2007; Kalakkunnath et al., 2005, 2006, 2007a,b) and comprehensive evaluation of membrane transport (Kusuma et al., 2008a; Lin and Freeman, 2005b, 2006a; Lin et al., 2005c, 2006e, 2007), a series of material design rules have emerged that provide a useful framework for the formulation of tailored PEO membranes for specific gas separations.

* Corresponding author. Tel.: +1 859 257 5507; fax: +1 859 323 1929.
E-mail address: kalika@engr.uky.edu (D.S. Kalika).

0009-2509/$ - see front matter © 2008 Elsevier Ltd. All rights reserved.
doi:10.1016/j.ces.2008.11.026

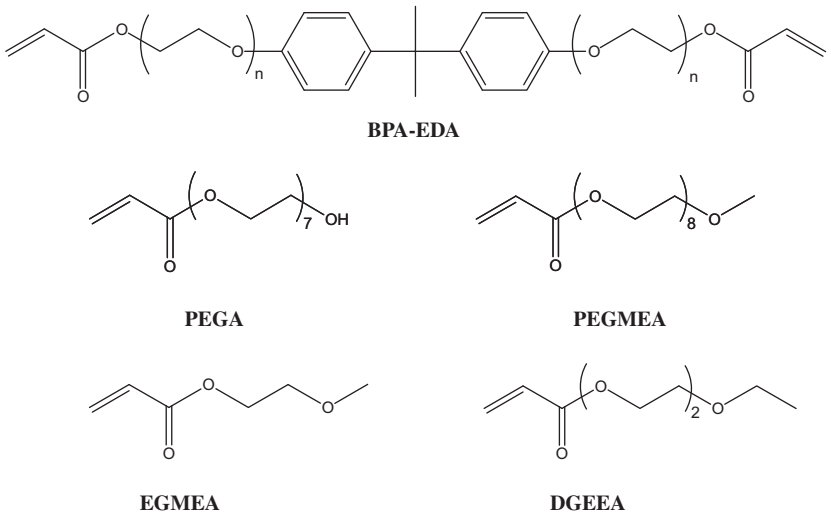

Fig. 1. Chemical structures of bisphenol A ethoxylate diacrylate (BPA–EDA) crosslinker ($n = 2$, 4, 15); poly(ethylene glycol) acrylate (PEGA), poly(ethylene glycol) methyl ether acrylate (PEGMEA), ethylene glycol methyl ether acrylate (EGMEA), diethylene glycol ethyl ether acrylate (DGEEA) co-monomers.

The permeability of gas molecules through a polymer membrane reflects both penetrant solubility and diffusivity in the polymer (Matteucci et al., 2006). In rubbery polymers, solubility depends primarily on the condensability of the gas, as well as on interactions between the gas molecules and the polymer matrix. Diffusivity is governed by the relative size of the penetrant and the free volume characteristics of the polymer. Synthetic strategies seeking to optimize gas separation properties (e.g., CO_2 permeability; CO_2/light gas selectivity) can be designed to improve either solubility selectivity, diffusivity selectivity, or both. For example, we have examined a series of networks based on PEGDA crosslinker copolymerized with acrylates of similar chemical composition (i.e., poly(ethylene glycol) methyl ether acrylate (PEGMEA) and poly(ethylene glycol) acrylate (PEGA)) (Lin et al., 2006e). The introduction of mono-functional acrylate in the pre-polymerization mixture leads to the insertion of fixed-length pendant groups along the network backbone and a corresponding decrease in the effective crosslink density. In the case of the PEGDA/PEGMEA series of copolymers, it was observed that the presence of flexible $–OCH_3$ terminated side chains produced a systematic increase in fractional free volume (FFV) that was responsible for a five-fold enhancement in CO_2 permeability owing to an increase in penetrant diffusivity. For this particular series of copolymers, the relative EO contents of the crosslinker and side chains were similar, such that CO_2 solubility was largely unchanged as a function of copolymer composition. More recently, the properties of PEGDA-based networks incorporating short-chain pendant groups have been studied in order to assess the potential efficacy of these moieties in enhancing local free volume and corresponding permeability (Borns et al., 2007; Kusuma et al., 2008a).

The relatively straightforward chemical synthesis afforded by the UV polymerization of flexible PEG acrylates presents a wide range of chemical and structural options for the formulation of CO_2-selective gas separation membranes. In this paper, a series of membrane copolymers are examined based on the photopolymerization of bisphenol A ethoxylate diacrylate (BPA–EDA); see Fig. 1. The BPA–EDA crosslinker contains symmetric $–(CH_2CH_2O)_n–$ repeat segments and a central bisphenol A linkage that frustrates chain packing and limits potential crystallization. Homopolymer and copolymer networks were prepared using three different BPA–EDA molecular weights ($n = 2$, 4, and 15); acrylate co-monomers included PEGMEA and PEGA, as well as lower molecular weight PEG analogs intended to introduce shorter pendants along the backbone (i.e., EGMEA and DGEEA, see Fig. 1). The objective of the study is to assess the influence of systematic changes in polymer crosslink density and composition on the static and dynamic properties of the networks, and their relation to gas separation performance. Dynamic mechanical analysis and dielectric spectroscopy are used to elucidate the molecular relaxations of the crosslinked networks, and their permeability and solubility characteristics are measured for a series of relevant gases; the results are discussed relative to the properties of the XLPEGDA model polymer networks described above, as well as in comparison to analogous networks based on bisphenol A ethoxylate dimethacrylates as studied by Hirayama et al. (1999). This detailed evaluation as to the impact of controlled modifications of network architecture on the properties of the BPA–EDA polymers provides fundamental insight regarding the relationships between network structure, dynamics, and gas transport in these materials, as well as an appraisal of selected synthetic strategies for the enhancement of separation performance.

2. Experimental

2.1. Materials

BPA–EDA crosslinker was obtained in three molecular weights corresponding to EO repeat lengths of $n = 2$, 4, and 15 (refer to Fig. 1). BPA–EDA monomers with nominal molecular weights equal to 512 g/mol ($n = 2$) and 688 g/mol ($n = 4$) were obtained from Aldrich Chemical Company (Milwaukee, WI). BPA–EDA monomer with molecular weight equal to 1656 ($n = 15$) was obtained from Sartomer Company (Exton, PA). The acrylate co-monomers were also obtained from Aldrich: poly(ethylene glycol) methyl ether acrylate (PEGMEA: MW = 460 g/mol); poly(ethylene glycol) acrylate (PEGA: MW = 380 g/mol); ethylene glycol methyl ether acrylate (EGMEA: MW = 130 g/mol); and diethylene glycol ethyl ether acrylate (DGEEA: MW = 188 g/mol). 1-hydroxyl-cyclohexyl phenyl ketone (HCPK) was the photoinitiator. All reagents were used as received.

Gas cylinders of methane (99% purity) and carbon dioxide, hydrogen, nitrogen and oxygen (99.9% purity) were purchased from Airgas Southwest, Inc. (Corpus Christi, TX) and were used as received.

2.2. Monomer characterization

Proton nuclear magnetic resonance (^{1}H NMR) was used to confirm the molecular weights of the as-received BPA–EDA crosslinkers

(Lin et al., 2005c). Samples were prepared by dissolving dry BPA–EDA monomers in $CDCl_3$ (99.6 D%) obtained from Aldrich Chemical Company, at concentrations between 5 and 10 wt%. ^{1}H NMR spectra were recorded on a VARIAN INOVA-500 spectrometer operating at 600 MHz, and the data are reported here in ppm relative to the $CDCl_3$ solvent peak at δ 7.24 (Gottlieb et al., 1997). The spectrometer was adjusted routinely as follows: spin rate, 20 rpm; pulse width, 2.0 μs; sweep width, 9615 Hz; line broadening (with exponential multiplication), 0.1 Hz with 128 K data points. The relaxation delay was 24 s (i.e., $5T_1$). The peaks are described as follows: ^{1}H NMR ($CDCl_3$): δ 7.06 and δ 6.75 (4 H each, *m* and *o* hydrogen atoms in phenyl rings of bisphenol-A relative to EO chain), δ 6.38, δ 6.11, and δ 5.79 (2 H each, *cis*, *gem*, and *trans* hydrogen atoms relative to –C(═O)–O– in CH_2═CHR acrylate end-group), δ 4.27 and δ 3.70 (4 H each, α and β hydrogen atoms in closest CH_2–CH_2–O relative to acrylate group), δ 4.05 and δ 3.79 (4 H each, α and β hydrogen atoms in closest CH_2–CH_2–O relative to bisphenol-A group), δ 3.60 ($8\times(n-2)$ H in CH_2–CH_2–O not immediately adjacent to acrylate or bisphenol-A groups), and δ 1.58 (6 H, β hydrogen atoms flanked by the two phenyl rings).

The molecular weight of BPA–EDA can be confirmed by taking the ratio of the δ 3.60 peak integral (originating from the hydrogen atoms in the middle of the EO chain) to that of any of the other peaks; this approach has been used previously to confirm the molecular weight of PEGDA (Lin et al., 2005c). For the BPA–EDA ($n = 2$) crosslinker, it is expected that the δ 3.60 peak would be absent, according to the peak assignments presented above. Analysis of the experimental spectra verified the molecular weight of the BPA–EDA monomers as consistent with the specifications of the suppliers.

2.3. Film preparation

Crosslinked polymer films were prepared via UV photopolymerization; a detailed description of the polymerization method is provided in Kalakkunnath et al. (2005). Pre-polymerization blends of BPA–EDA crosslinker and the selected acrylate co-monomer were formulated in the desired proportions in combination with 0.1 wt% HCPK initiator. The mixture was sandwiched between parallel quartz plates with controlled spacing and exposed to 312 nm UV light for 90 s at 3 mW/cm^2. Thickness of the resulting crosslinked films was ~1.0 mm for the dynamic mechanical specimens and ~0.35 mm for the dielectric specimens. For gas transport measurements, the film thickness was varied from 0.50 mm for the most permeable copolymer films based on BPAEDA15, down to 0.07 mm for the least permeable films based on BPAEDA4. The exact thickness of each film was determined using a digital micrometer with precision to ± 1 μm.

Attenuated total reflection Fourier transform infrared spectroscopy (FTIR–ATR) was used to evaluate the degree of conversion of acrylate groups in the solid films (see Lin et al., 2005c for experimental details). The disappearance of acrylate double bonds due to polymerization leads to a decrease in sharp peaks at 810 and 1410 cm^{-1} associated with the CH_2═CH groups (Colthup et al., 1975), and these were monitored in order to assess the extent of reaction. The carbonyl band at 1725 cm^{-1} was used as a reference to facilitate comparison of the spectra.

Bulk density measurements of the crosslinked polymer films were conducted at 25 °C using a conventional density determination kit (Denver Instruments, CO); *n*-heptane was employed as the auxiliary liquid. FFV in the polymers was calculated based on the measured density according to the approach described previously (Lin et al., 2006e; see also Kusuma et al., 2008a), with specific occupied volume estimated via Bondi group contribution methods (Van Krevelen, 1990).

2.4. Dynamic mechanical analysis

Dynamic mechanical analysis was performed using a Polymer Laboratories DMTA operating in single cantilever bending geometry. The films had a thickness of ~1.0 mm and were held under vacuum at room temperature for at least 24 h prior to measurement. The sample mounting procedures were designed to minimize exposure to ambient moisture. Storage modulus (E') and loss tangent ($\tan\delta$) were measured at a heating rate of 1 °C/min with test frequencies of 0.1, 1, and 10 Hz. All experiments were carried out under an inert (N_2) atmosphere.

2.5. Dielectric relaxation spectroscopy

Dielectric spectroscopy measurements were conducted using the Novocontrol "Concept 40" broadband dielectric spectrometer (Hundsangen, Germany). Dielectric constant (ε') and loss (ε'') were recorded in the frequency domain (0.1 Hz to 1 MHz) at 4 °C isothermal intervals from −150 to 100 °C. In order to optimize electrical contact during measurement, concentric silver electrodes were deposited on each polymer sample using a VEECO thermal evaporation system. Samples were subsequently mounted between gold platens and positioned in the Novocontrol Quatro Cryosystem. Each sample was dried under vacuum at room temperature prior to measurement; thickness was ~0.35 mm in all cases.

2.6. Transport measurements

Pure gas permeability measurements (CO_2, CH_4, H_2, N_2, and O_2) were completed at 35 °C using a constant volume/variable pressure apparatus as described previously (Lin and Freeman, 2004, 2006b). Gas flux and permeability were calculated from the pressure rise in a pre-evacuated downstream vessel of known fixed volume. The samples were partially masked with impermeable aluminum tape applied on the upstream face of the membrane in order to accurately define the surface area available for gas transport. In all cases, the downstream pressure was < 2 cm-Hg, which was very low relative to the range of upstream pressures applied (4–15 atm). In order to compare the inherent permeability of each polymer to various gases, the measured values were extrapolated to an upstream pressure equal to 0; the reported values ($P_{A,o}$) correspond to penetrant permeability at infinite dilution (Lin and Freeman, 2004).

Pure gas solubility measurements (CO_2 and CH_4) were performed at 35 °C using a dual-volume, dual-transducer apparatus based on the barometric pressure-decay method (Kusuma et al., 2008a; Lin and Freeman, 2004). The samples were degassed overnight in a vacuum oven prior to mass and density measurements to remove residual water vapor absorbed from the atmosphere (Kusuma et al., 2008a). Gas diffusivity was calculated based on experimental permeability and solubility values, assuming the solution–diffusion model of gas transport through a dense polymer film (Baker, 2004).

3. Results and discussion

3.1. Properties of polymer networks

UV photopolymerization of the BPA–EDA crosslinker led to the formation of wholly-amorphous networks. For the higher molecular weight crosslinkers ($n = 4$,15; see Fig. 1), the effective distance between crosslinks was sufficiently large that rubbery networks were produced (i.e., $T_g < 25$ °C), while for the $n = 2$ crosslinker, a glassy solid was obtained. Dynamic mechanical glass transition temperatures (T_α; 1 Hz) for the networks are reported in Table 1. FTIR–ATR was used to monitor the degree of acrylate conversion in the polymer films by following the disappearance of characteristic

Table 1
Characteristics of crosslinked BPA–EDA copolymer networks.

	T_α (1 Hz)[a]	β_{KWW}[b]	FFV[c]
XLBPAEDA2	43	0.16	0.119
BPAEDA2/PEGMEA			
80/20	41	0.15	0.117
60/40	9	0.17	0.122
50/50	−11	0.16	0.126
40/60	−23	0.17	0.130
BPAEDA2/PEGA			
80/20	38	0.15	0.114
60/40	16	0.15	0.116
50/50	3	0.14	0.117
40/60	−6	0.13	0.119
XLBPAEDA4	11	0.21	0.118
BPAEDA4/PEGMEA			
80/20	−8	0.21	0.122
60/40	−24	0.21	0.126
50/50	−30	0.19	0.127
BPAEDA4/PEGA			
80/20	−2	0.21	0.119
60/40	−15	0.20	0.118
50/50	−21	0.19	0.119
XLBPAEDA15	−34	0.28	0.125
BPAEDA15/PEGMEA			
90/10	−36	0.28	0.126
80/20	−39	0.29	0.128
70/30	−41	0.28	0.130
60/40	−44	–	0.132
BPAEDA15/DGEEA			
90/10	−36	0.29	0.127
80/20	−38	0.29	0.131
70/30	−38	0.28	0.135
60/40	−38	0.29	0.138
BPAEDA15/EGMEA			
90/10	−34	0.30	0.128
80/20	−33	0.29	0.130
70/30	−31	0.28	0.133
60/40	−30	0.29	0.135

[a] T_α (°C) is the dynamic mechanical peak temperature at 1 Hz.
[b] β_{KWW} is the Kohlrausch–Williams–Watts distribution parameter.
[c] FFV is the estimated fractional free volume based on bulk density measurements at 25 °C. All copolymer compositions are reported on a wt% basis.

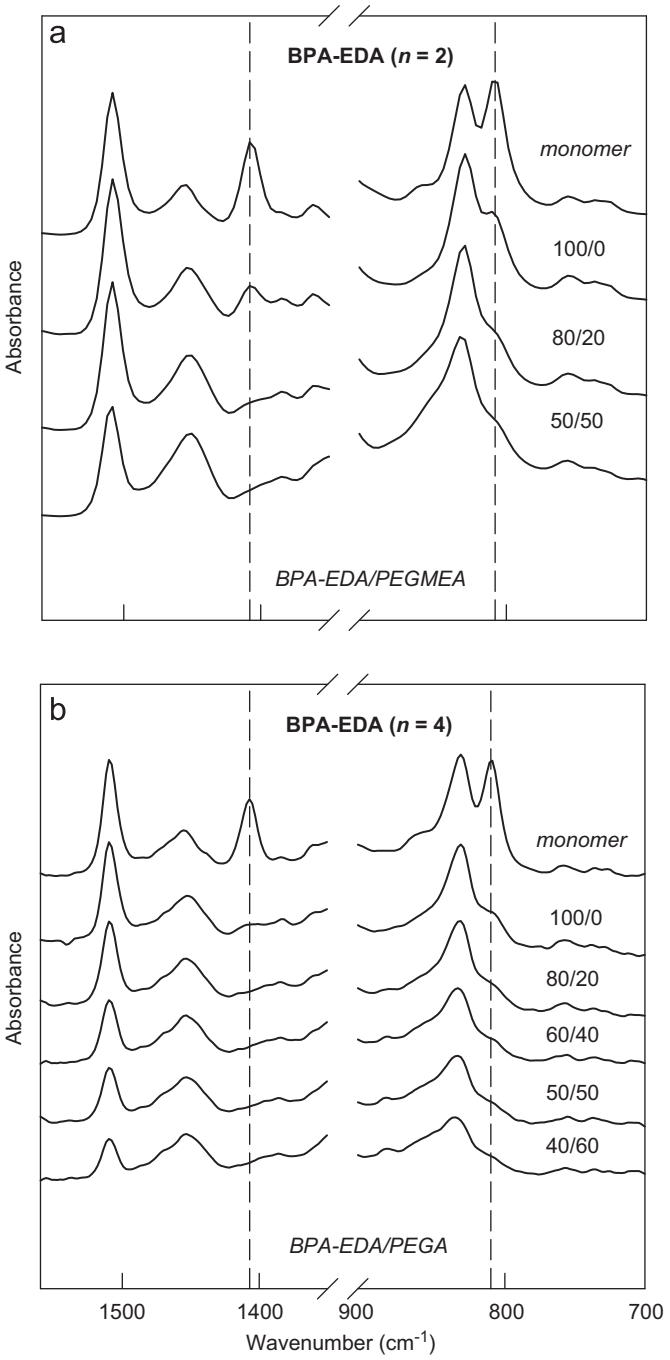

Fig. 2. FTIR spectra of BPA–EDA liquid monomer and solid crosslinked copolymer films: (a) BPA–EDA ($n = 2$) crosslinker and BPAEDA2/PEGMEA copolymers and (b) BPA–EDA ($n = 4$) crosslinker and BPAEDA4/PEGA copolymers. All copolymer compositions reported on a wt% basis.

absorbance peaks at 810 and 1410 cm^{-1}; spectra for the monomers and networks based on the $n = 2$ and 4 crosslinkers are presented in Fig. 2. In the case of the XLBPAEDA2 network (i.e., homopolymer based on the $n = 2$ crosslinker), comparison of the network spectrum with that of the liquid monomer indicates the presence of residual acrylate groups that are not fully converted under the reaction conditions. As the incipient network emerges, the relatively short crosslink bridges associated with the $n = 2$ monomer limit chain mobility and the network eventually vitrifies as the reaction proceeds. The remaining CH_2═CH groups in the polymer are most likely present as dangling chain ends. For the XLBPAEDA4 network, which remains rubbery throughout the polymerization process, examination of the IR absorbance at 810 cm^{-1} also indicates a small amount of residual acrylate present. In both the XLBPAEDA2 and XLBPAEDA4 networks, copolymerization with flexible PEGMEA or PEGA monomers leads to a reduction in the effective glass transition temperature of the polymer, and the reaction is able to proceed under conditions of much greater molecular mobility. As a result, virtually 100% acrylate conversion is obtained for these materials (*re*: copolymer spectra in Fig. 2). Homopolymer and copolymer networks prepared from the BPAEDA15 monomer also displayed complete conversion of the acrylate groups owing to the flexibility of the crosslinker and the low glass transition temperature of the final network (*spectra not shown*); this result is consistent with polymerization studies completed on PEGDA crosslinker (nominal MW of 700 g/mol with n∼14 EO units) prepared under the same reaction conditions (Lin et al., 2005c).

The crosslinked polymers were subsequently characterized by dynamic mechanical analysis and dielectric spectroscopy, as well as

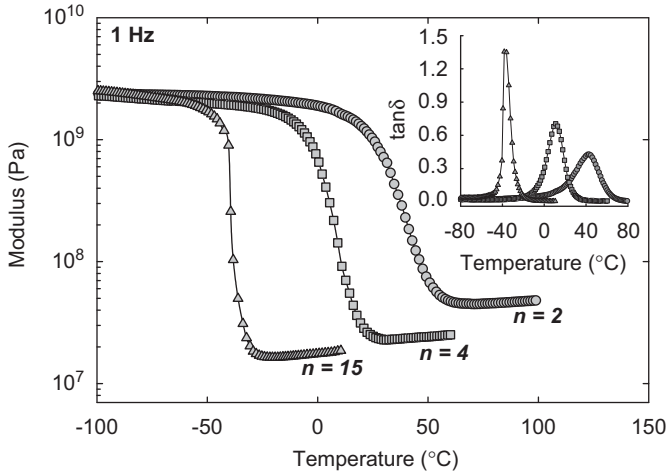

Fig. 3. Storage modulus (E'; Pa) vs. temperature (°C) for XLBPAEDA networks. Frequency of 1 Hz; heating rate of 1 °C/min. *Inset*: tan δ vs. temperature.

transport measurements. In all cases, the homopolymer and copolymer network films were tested as-prepared, with no additional steps taken to influence the acrylate conversion (Kalakkunnath et al., 2006).

3.2. Dynamic mechanical analysis

Dynamic mechanical results for the homopolymer networks based on BPA–EDA are presented as storage modulus (E') vs. temperature at 1 Hz in Fig. 3. The glass–rubber relaxation is indicated by an approximately two order of magnitude drop in modulus with an accompanying maximum in tan δ (*see inset*). The glass transition temperature (T_α; determined from the peak in tan δ at 1 Hz) shifts to higher values with decreasing distance between crosslinks, consistent with prior studies on PEO networks synthesized from PEGDA (Kalakkunnath et al., 2006). It is worth noting that for the XLBPAEDA15 network, which contains crosslink bridges encompassing 30 EO units plus a central BPA linkage, the value of T_α is essentially the same as that obtained previously for XLPEGDA14 networks with 14 EO units between crosslink junctions ($T_\alpha = -35$ °C).

The molecular weight of the crosslinker has little influence on the value of the storage modulus in the glassy region. Above T_g, the rubbery modulus increases systematically with effective crosslink density in a manner that is consistent with classical elasticity theory (*re*: Fig. 3) (Treloar, 1975). In addition, the relaxation breadth increases markedly with crosslink density (i.e., at lower BPA–EDA molecular weight), as the conformational constraints imposed by the covalent crosslink junctions produce an increasingly heterogeneous relaxation response. Examination of the tan δ vs. temperature curve for the XLBPAEDA2 network (inset of Fig. 3) reveals an especially broad relaxation that includes a weak low-temperature shoulder that may reflect contributions from dangling residual chain ends present in the sample.

As discussed above, a number of copolymer formulations have been explored in an effort to understand the influence of varying chain architecture on the thermomechanical properties of the networks and their corresponding gas transport performance. By copolymerizing the BPA–EDA crosslinker with EO-based acrylates, it is possible to preserve the desired polar character of the resulting network while at the same time controlling crosslink density and free volume via the insertion of side pendants with varying length and terminal groups. For the lower molecular weight crosslinkers ($n = 2$, 4), relatively long PEGMEA and PEGA co-monomers were introduced

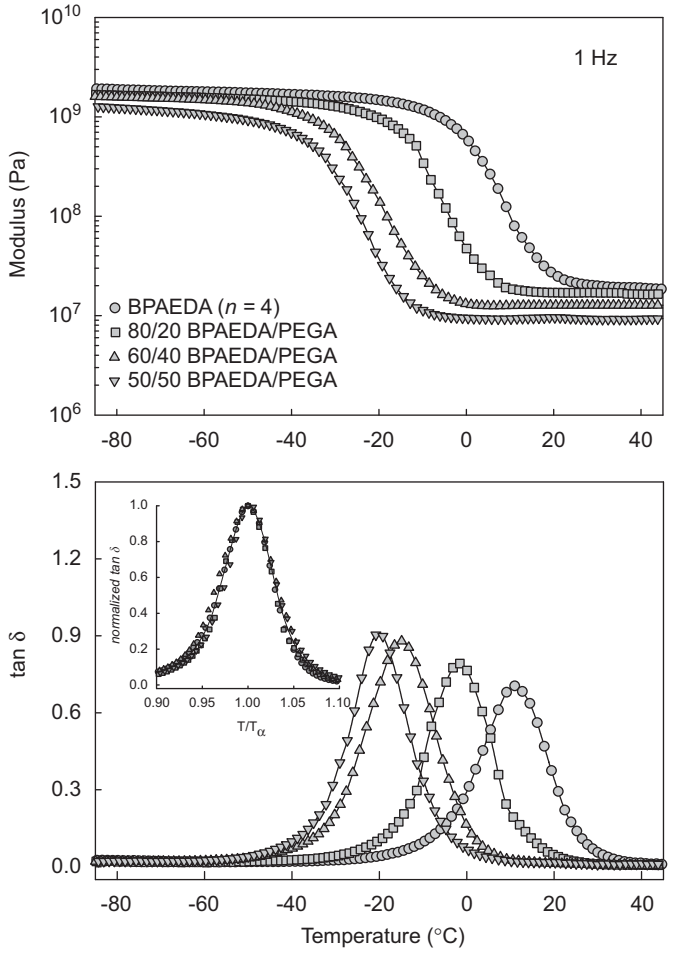

Fig. 4. Dynamic mechanical properties (E'; tan δ) vs. temperature (°C) for BPA–EDA/PEGA copolymer networks; BPA–EDA ($n = 4$) crosslinker. Frequency of 1 Hz; heating rate of 1 °C/min. *Inset*: normalized tan δ vs. temperature at 1 Hz.

into the reaction mixture as a means to both increase the overall flexibility of the network and enhance EO content. Representative dynamic mechanical results for these copolymers (BPAEDA4/PEGA networks) are presented in Fig. 4. The introduction of the PEGA co-monomer leads to a progressive decrease in the glass transition temperature of the networks and a reduction in rubbery modulus that reflects the stoichiometrically-controlled decrease in effective crosslink density. For both the BPAEDA2 and BPAEDA4 crosslinkers, the reduction in T_g observed with increasing co-monomer content was stronger upon the insertion of $-OCH_3$ terminated PEGMEA groups as compared to –OH terminated PEGA (see Table 1).

The copolymer formulations prepared using the BPAEDA15 crosslinker were limited to co-monomers containing $-OCH_3$ or $-OC_2H_5$ terminal groups, as these moieties were found to be most effective in increasing network free volume and enhancing gas permeability in studies on PEGDA-based membranes (Kusuma et al., 2008a; Lin et al., 2006e). The glass transition temperatures of the BPAEDA15 copolymers are presented in Table 1. Here again, insertion of the relatively long PEGMEA chains along the network backbone produced a decrease in glass transition temperature, although this effect was somewhat muted given the already inherently flexible character of the BPAEDA15 crosslinker. In addition, the inclusion of $\geqslant 40$ wt% PEGMEA in the BPAEDA15/PEGMEA copolymers led to the observation of crystallization in the networks as evidenced by cold-crystallization and melting events during the course of the

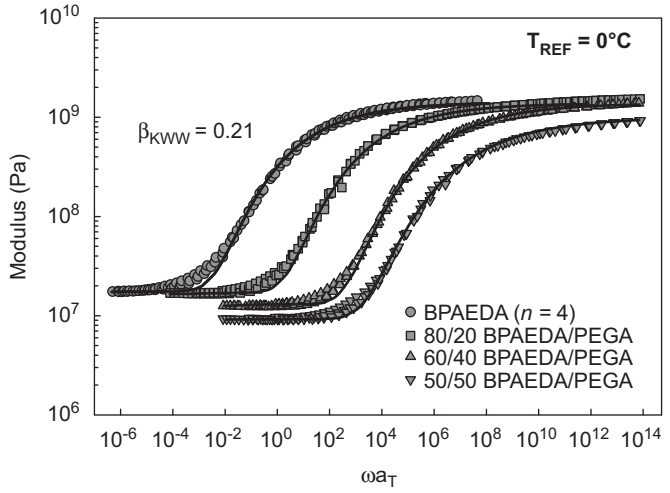

Fig. 5. Time–temperature master curves (E' vs. ωa_T) for BPA–EDA/PEGA copolymer networks; BPA–EDA ($n = 4$) crosslinker. Reference temperature of 0 °C. Solid curves from KWW equation.

dynamic mechanical heating sweeps. Introduction of short-branch pendants (i.e., EGMEA co-monomer) led to a modest stiffening of the network backbone as manifested in higher T_α values across the copolymer series. For the medium-length DGEEA co-monomer, a small decrease in glass transition temperature was observed for the various copolymer compositions. Both trends are consistent with prior measurements on PEGDA copolymers (Borns et al., 2007).

An important physical characteristic related to both the thermal and transport properties of these networks is FFV. FFV was estimated based on bulk density measurements of the polymers at 25 °C. Values for the homopolymer and copolymer networks are reported in Table 1. Introduction of the methyl-terminated PEGMEA co-monomer led to a progressive enhancement in FFV for all three crosslinkers, most likely reflecting a combination of decreasing crosslink density and the presence of local defects created by inserting the $-OCH_3$ terminated pendants into the surrounding hydrophilic matrix. An even greater increase in FFV was observed with the incorporation of the short-branch (methyl-terminated) EGMEA and (ethyl-terminated) DGEEA co-monomers in XLBPAEDA15. The lack of a similar effect upon copolymerization with the –OH terminated PEGA co-monomer has been attributed to the potential formation of hydrogen bonds involving the hydroxyl end groups (Borns et al., 2007; Kalakkunnath et al., 2005).

In order to further characterize the dynamic mechanical glass–rubber relaxation properties of the networks, time–temperature superposition was used to construct master curves of storage modulus vs. frequency (Ferry, 1980); representative results for the BPAEDA4/PEGA series of networks is presented in Fig. 5. The data can be described using the Kohlrausch–Williams–Watts (KWW) stretched exponential function, with the relative breadth of the relaxation quantified in terms of the exponent, β_{KWW}. Values of β_{KWW} range from 0 to 1, with $\beta_{KWW} = 1$ corresponding to a single relaxation time Debye response. Lower values of β reflect relaxation broadening due to intermolecular coupling as well as inhomogeneities arising from chemical or physical crosslinks (Roland, 1994; Schroeder and Roland, 2002). Series approximations for the KWW function express storage modulus in the frequency domain, and these equations were used as the basis for best-fit determinations of β_{KWW} (Williams et al., 1971). KWW curve fits for the BPAEDA4/PEGA series are shown in Fig. 5.

The KWW exponents for the various homopolymer and copolymer networks are reported in Table 1. For the homopolymers, β_{KWW} drops from 0.28 to 0.16 with decreasing distance between crosslinks, reflecting a progressively more constrained relaxation environment for the longer-range segmental motions associated with the glass transition; the broadening captured in the values of β_{KWW} is consistent with the shape of the tan δ curves, as shown in Fig. 3. The β_{KWW} value for the relatively unconstrained XLBPAEDA15 network is nearly the same as that measured for XLPEGDA14 ($\beta_{KWW} = 0.30$) (Kalakkunnath et al., 2006). Across the various BPA–EDA copolymer series, there is little variation in the KWW exponent with increasing co-monomer content. Previous studies on PEGDA/PEGMEA and PEGDA/PEGA copolymers revealed a narrowing of the glass transition (i.e., increasing β_{KWW} value) with increasing co-monomer content (Kalakkunnath et al., 2005). This was attributed to decreasing overall crosslink density, and to the fact that the flexible $-(CH_2CH_2O)-$ backbone of the PEGMEA and PEGA side groups was identical to the crosslinker repeat segment. In the case of the XLBPAEDA copolymer networks, the somewhat disparate character of the BPA–EDA crosslinker as compared to the co-monomers may be responsible for a modest increase in heterogeneity, thus offsetting the narrowing influence of reduced crosslink density and increasing network flexibility. The net result is relaxations of similar breadth across the various copolymer series, as demonstrated by the shape of the normalized loss curves shown in the inset of Fig. 4.

3.3. Dielectric relaxation spectroscopy

Broadband dielectric spectroscopy serves as a valuable complement to dynamic mechanical analysis in that it offers a very wide range of experimental test frequencies and is often more effective in probing local sub-glass motions that typically have only a weak influence on the bulk mechanical properties of the polymer. Previously, we have reported detailed dielectric investigations of the sub-glass and glass–rubber relaxation processes of PEO networks based on PEGDA crosslinker (Borns et al., 2007; Kalakkunnath et al., 2007a,b); the dielectric characteristics of the XLBPAEDA networks will be examined within the context of these prior studies. Further, the BPA–EDA monomers afford an opportunity to evaluate the influence of crosslinker molecular weight on the dielectric relaxation response of the materials.

Dielectric results for the XLBPAEDA homopolymer networks are presented as dielectric constant (ε') and loss (ε'') vs. temperature at 120 kHz in Fig. 6. The data show two transitions with increasing temperature that are each evident as a step-wise increase in dielectric constant and a corresponding maximum in dielectric loss: a merged sub-glass (β) process, and the glass–rubber (α) relaxation. The positions and relative breadth of the dielectric glass–rubber relaxations for the three BPA–EDA crosslinkers are consistent with the dynamic mechanical data presented in Fig. 3.

A detailed view of the dielectric loss response for the BPA–EDA homopolymers in the sub-glass region (−78 °C) is presented in Fig. 7. For all three crosslinkers, two overlapping sub-glass relaxations are observed that have been labeled according to their position with respect to increasing temperature: the lower-temperature (β_1) relaxation appears on the high frequency side of the spectrum, while the higher-temperature (β_2) relaxation appears at lower frequencies. The positions of both sub-glass relaxations are close to those observed for the XLPEGDA14 network (Kalakkunnath et al., 2007b), as well as for crystalline PEO (Jin et al., 2002), and are nearly independent of crosslinker molecular weight. The β_1 relaxation has been interpreted as a typical sub-glass process originating from localized EO motions, while the β_2 relaxation has been identified as a "fast", non-cooperative segmental process that originates in the vicinity of the crosslink junctions and which is sensitive to the degree of crosslinking in the network (Borns et al., 2007; Kalakkunnath et al., 2007a,b).

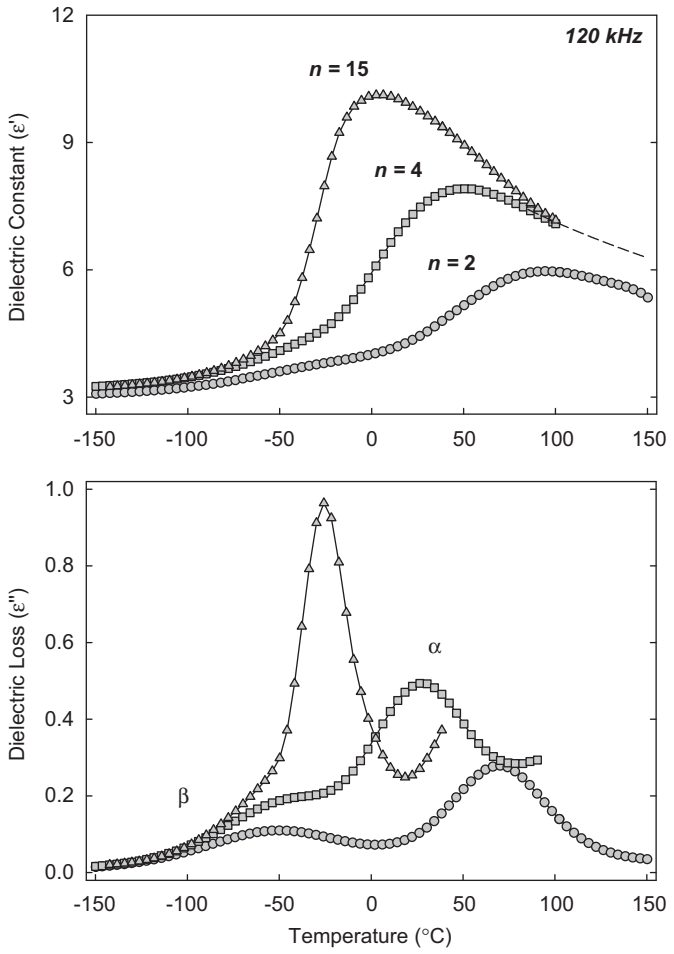

Fig. 6. Dielectric constant (ε') and loss (ε'') vs. temperature (°C) for XLBPAEDA homopolymer networks. Frequency of 120 kHz.

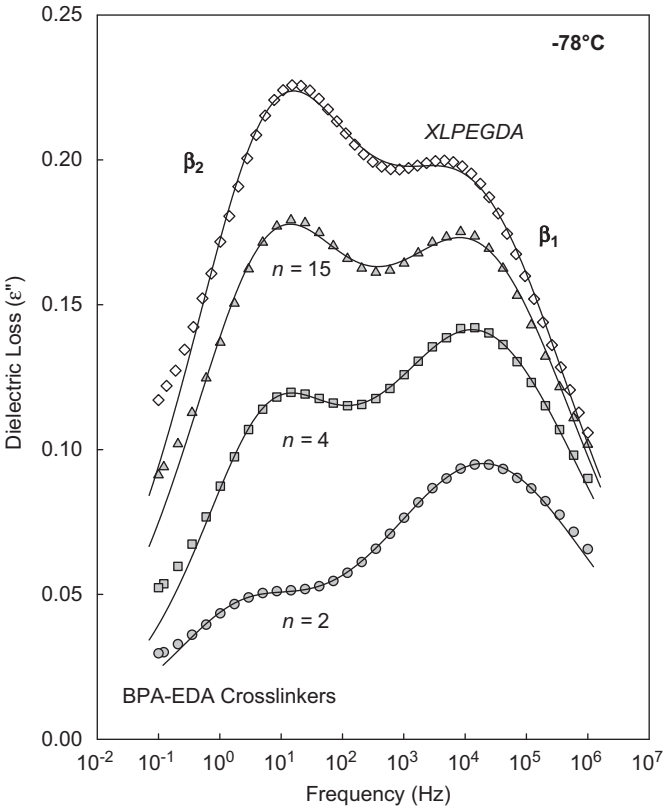

Fig. 7. Dielectric loss (ε'') vs. frequency (Hz) for XLBPAEDA homopolymer networks at −78 °C. XLPEGDA14 data reported from Kalakkunnath et al. (2007b). Solid curves are dual HN fits.

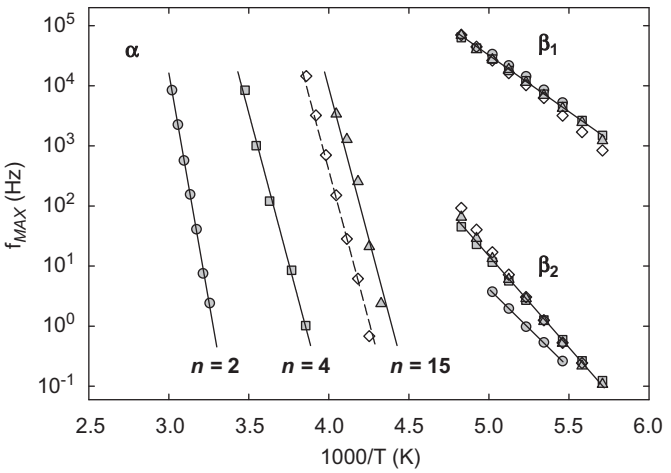

Fig. 8. Arrhenius plot of $f_{MAX} = (2\pi\tau_{MAX})^{-1}$ for XLBPAEDA homopolymer networks based on dielectric loss results (shaded symbols). XLPEGDA14 (◊) data reported from Kalakkunnath et al. (2007b).

The dielectric dispersions across the sub-glass region have been analyzed using a dual Havriliak–Negami (HN) expression (Havriliak and Negami, 1966); for details of the analysis see Kalakkunnath et al. (2007b). Both sub-glass relaxations could be described using the symmetric Cole–Cole form of the HN equation, and the resulting best-fit curves are included in Fig. 7. The relaxation time (τ_{MAX}) associated with each maximum in dielectric loss is plotted as $f_{MAX} = (2\pi\tau_{MAX})^{-1}$ vs. 1000/T (i.e., Arrhenius form) in Fig. 8. All data for the β_1 relaxation collapse onto a single line with an apparent activation energy, $E_A = 36$ kJ/mol. For the β_2 relaxation, the XLBPAEDA4 and XLBPAEDA15 data sets coincide with $E_A = 60$ kJ/mol, while the β_2 process in XLBPAEDA2 is offset to slightly higher temperatures. The similarity of the dielectric sub-glass relaxation times measured for the XLBPAEDA and XLPEGDA networks, as well as their invariance with respect to crosslinker molecular weight, is consistent with the localized character of the underlying motions responsible for these relaxations.

The intensity of the sub-glass relaxation processes, as shown in Fig. 7, increases with increasing crosslinker molecular weight for the XLBPAEDA networks. This response may be due to variations in the chemical constitution of the networks (i.e., number and type of constituent dipoles), as well as to possible changes in dipolar mobility owing to varying crosslink density. The measured relaxation intensity can be evaluated relative to variations in composition and potential dipolar correlation by application of the Kirkwood–Onsager equation (Froehlich, 1958):

$$\Delta\varepsilon = \varepsilon_R - \varepsilon_U = \left(\frac{\varepsilon_U + 2}{3}\right)^2 \left(\frac{3\varepsilon_R}{2\varepsilon_R + \varepsilon_U}\right) \frac{N}{3kT\varepsilon_o} \cdot g\mu_o^2 \quad (1)$$

where ε_R and ε_U represent the relaxed and unrelaxed values of the dielectric constant, N is the number density of dipoles within the polymer, μ_o is the uncorrelated dipole moment, and k and ε_o are the Boltzmann constant and permittivity of free space, respectively. The correlation factor (g) accounts for deviations from an isolated, unencumbered response for each constituent dipole, and g values

Table 2
Dielectric properties (−78 °C) for β_1 and β_2 sub-glass relaxations in homopolymer networks.

	$\Delta\varepsilon$ (β_1)[a]	$\Delta\varepsilon$ (β_2)[a]	g (β_1)[b]	g (β_2)[b]
XLBPAEDA2	0.69	0.16	0.10	0.02
XLBPAEDA4	1.00	0.41	0.12	0.04
XLBPAEDA15	1.08	0.82	0.12	0.07
XLPEGDA14	1.14	1.10	0.11	0.07

[a] $\Delta\varepsilon = \varepsilon_R - \varepsilon_U$ is the dielectric relaxation intensity.

[b] g corresponds to the Kirkwood–Onsager correlation factor.

< 1 typically reflect intra and intermolecular correlation, spatial restrictions, and possible dipolar cancellation.

The measured dielectric relaxation intensities for the two sub-glass relaxations ($\Delta\varepsilon = \varepsilon_R - \varepsilon_U$) are reported in Table 2. The Kirkwood–Onsager equation was used to calculate the correlation factor (g) for each relaxation. For the XLBPAEDA and XLPEGDA networks, two types of dipoles are present that can potentially contribute to the dipolar response: ester dipoles associated with the acrylate crosslink junctions and ether oxygen dipoles associated with the PEO repeat segments. The dipole moments assigned to these groups are 1.80D and 1.07D, respectively (Saiz et al., 1981; Diaz-Calleja and Riande, 1997). In situations where more than one type of dipole can contribute to the intensity associated with a relaxation, it is often difficult to establish the extent to which a particular dipolar entity is responsible for the measured response. In order to estimate the correlation factor for the β_1 and β_2 relaxations, we assume that both types of dipoles can contribute to the individual relaxations, and calculate a single g value for each dispersion based on the total population of dipoles present in the network. The results for each homopolymer network, as well as for XLPEGDA14, are presented in Table 2.

Examination of the g values associated with the β_1 process shows that the correlation factor for this relaxation remains nearly constant, regardless of molecular weight, and is essentially the same as for XLPEGDA14. This outcome suggests that the progressive increase in relaxation intensity observed for the β_1 relaxation (*re*: Fig. 7) can be explained solely on the basis of changes in dipolar composition, as long as contributions from both the ether oxygen and ester dipoles are accounted for. As molecular weight of the BPA–EDA crosslinker increases, there is a trade-off in the number of ether oxygen vs. ester dipoles, as well as a dilution in the relative fraction of non-polar BPA groups contained within the network. The result is an increase in overall dipolar density with increasing n value, and this is reflected directly in the net dipolar response.

Comparison of the relative intensity of the β_1 and β_2 relaxations across the homopolymer series reveals a systematic increase in the strength of the β_2 relaxation with increasing molecular weight that exceeds the enhancement in dielectric response attributed to changes in dipolar content. Previous dielectric studies on the various PEGDA-based copolymer networks have shown the β_2 process to be sensitive to the overall degree of crosslinking, with the underlying motions associated with the β_2 relaxation closely correlated to the character of the crosslink junctions and the degree of motional constraint that they impose (Kalakkunnath et al., 2007a). For the XLBPAEDA homopolymer networks, the β_2 process is strongly suppressed for the lowest molecular weight crosslinker and increases in intensity as the molecular weight between crosslink junctions increases (i.e., as the overall network constraint is loosened); this result is reflected in the values of the corresponding correlation factors in Table 2. For the highest molecular weight crosslinker ($n = 15$), the β_2 correlation factor is the same as that measured for XLPEGDA14.

The dielectric sub-glass relaxation properties of the copolymer networks based on BPA–EDA crosslinkers have been examined relative to our earlier studies on the PEGDA copolymers. In general, the sub-glass relaxation characteristics of the BPA–EDA copolymer networks follow the trends observed for the PEGDA copolymers: the position and activation energies associated with the individual sub-glass relaxations are largely independent of copolymer composition, while the relative intensities of the β_1 and β_2 processes reflect changes in dipolar content and network constraint consistent with previous observations. Given the close similarity in the results for these two families of materials, no additional sub-glass relaxation data are presented for the BPA–EDA copolymers; the reader is referred to Borns et al. (2007), Kalakkunnath et al. (2007a,b) for greater detail on the sub-glass relaxations in the PEO networks.

In addition to the insight obtained with respect to the sub-glass processes operative in these polymers, dielectric spectroscopy is also useful for studying the characteristics of the glass–rubber relaxation. Dielectric loss (120 kHz) for the XLBPAEDA homopolymer networks and BPAEDA/PEGMEA copolymers is plotted vs. temperature in Fig. 9. For the homopolymers, the relaxation times (τ_{MAX}) associated with the α process were obtained via HN curve fits at discrete temperatures in the vicinity of the glass transition. A representative result for the XLBPAEDA15 network is shown in Fig. 10. Here, the influence of low-frequency conduction was removed according to the method presented in Kalakkunnath et al. (2007b), and the data were fit using a dual-HN expression encompassing the α relaxation and a merged (β_1+β_2) sub-glass process. Time-temperature results (f_{MAX} vs. $1/T$) for the dielectric glass transition in all three homopolymer networks are presented in Fig. 8. The range of data that could be reliably obtained from the HN fits was limited by the high conduction intensity encountered at the lowest test frequencies, and by strong overlap of the α and β relaxations at high frequencies. Across the range of accessible data, all three homopolymers display linear Arrhenius behavior, with a corresponding apparent activation energy, $E_A = 280$ kJ/mol. The results for XLPEGDA14 are also included in Fig. 8, and indicate a similar value for E_A.

Examination of the dielectric loss sweeps presented in Fig. 9 shows the strong variation in relaxation breadth and glass transition temperature encountered in the BPAEDA/PEGMEA copolymer networks. For the BPAEDA2 crosslinker, the inclusion of flexible PEGMEA branches appears to create two broadly overlapping relaxation environments that reflect the difference in inherent mobility between the constrained crosslink bridges and the flexible PEGMEA groups. For the XLBPAEDA4 networks, a more homogeneous relaxation environment is evident from the loss curves, but with the introduction of PEGMEA still driving a strong downward trend in T_g. Finally, for the copolymer networks based on BPAEDA15, a much narrower relaxation response is observed with minimal variation in glass transition temperature.

For those copolymer series that encompass only a small shift in T_g as a function of composition, dielectric spectra for the various copolymers can be compared directly in the frequency domain at a fixed temperature. Fig. 10 shows conduction-corrected results for the BPAEDA15/DGEEA copolymer series at −38 °C; the solid curves are dual-HN fits (Borns et al., 2007; Kalakkunnath et al., 2007a). The α relaxation peak for the copolymers shifts to higher frequencies (i.e., lower values of τ_{MAX}) as compared to the XLBPAEDA15 homopolymer, a result that is consistent with the modest downward offset in dynamic mechanical peak temperatures reported for this series in Table 1. The strong increase in relaxation intensity observed for the glass–rubber relaxation is due to an increase in the net dipolar content of the network with increasing co-monomer. As the amount of DGEEA acrylate increases, the relative proportion of –COO– dipoles ($\mu = 1.8$D) increases as compared to both the number of $-CH_2CH_2O-$ groups ($\mu = 1.07$D) and (non-polar) BPA linkages. This trend is wholly-consistent with the results obtained for short-branch PEGDA networks as reported previously (Borns et al., 2007).

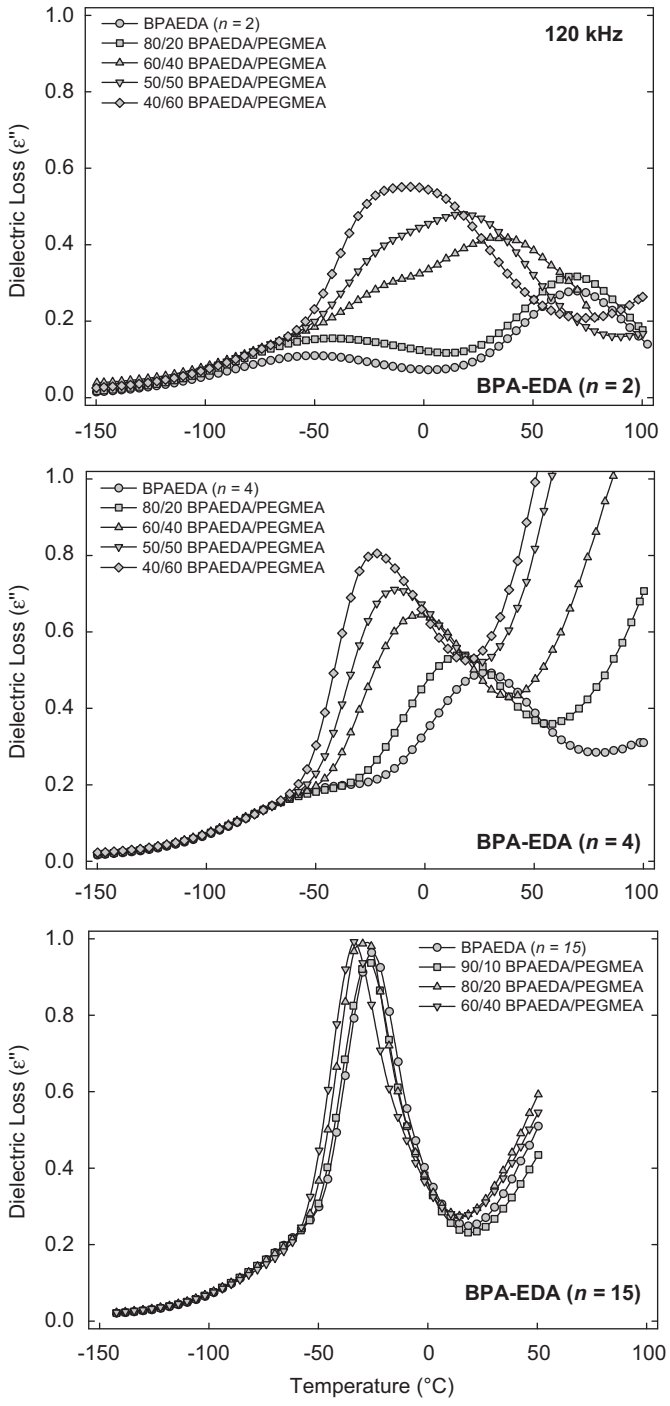

Fig. 9. Dielectric loss (ε'') vs. temperature (°C) for crosslinked BPAEDA/PEGMEA copolymer networks. Frequency of 120 kHz.

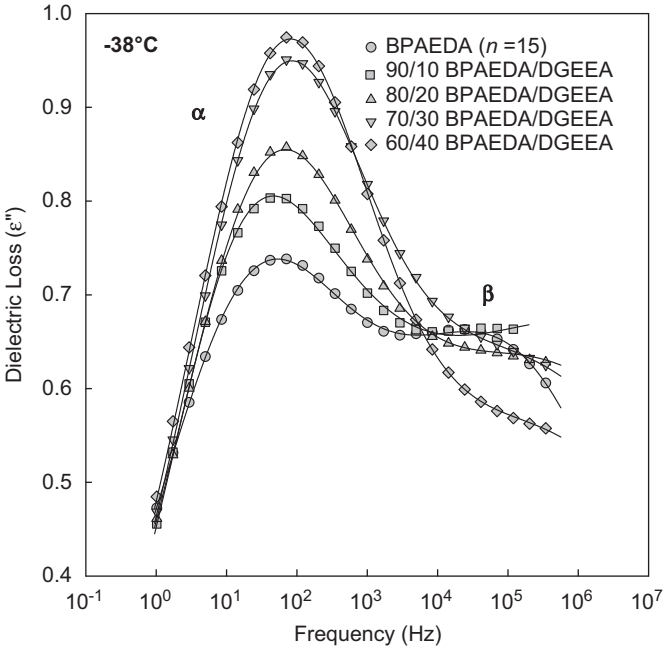

Fig. 10. Dielectric loss (ε'') vs. frequency (Hz) at −38 °C for crosslinked BPAEDA/DGEEA copolymer networks based on BPA–EDA ($n = 15$). Solid curves are dual HN fits.

Table 3
Pure gas permeability at 35 °C and infinite dilution.

	$P_{A,o}$ (Barrer)[a]				
	CO_2	H_2	CH_4	N_2	O_2
XLBPAEDA4	12	5.3	0.6	0.2	0.9
85/15 BPAEDA4/PEGMEA	23	8.3	1.1	0.4	1.6
70/30 BPAEDA4/PEGMEA	54	12	3.1	1.2	3.2
50/50 BPAEDA4/PEGMEA	132	20	8.4	3.0	7.5
25/75 BPAEDA4/PEGMEA	288	30	17	5.6	14
XLBPAEDA15	152	20	8.3	2.8	7.3
80/20 BPAEDA15/PEGMEA	198	24	11	3.5	9.3
70/30 BPAEDA15/PEGMEA	221	26	13	4.2	11
60/40 BPAEDA15/PEGMEA	261	28	15	4.7	12
50/50 BPAEDA15/PEGMEA	300	31	19	5.9	15
80/20 BPAEDA15/DGEEA	197	26	13	4.0	11
70/30 BPAEDA15/DGEEA	205	28	14	4.8	12
60/40 BPAEDA15/DGEEA	252	33	17	5.8	14
50/50 BPAEDA15/DGEEA	270	37	19	5.9	15
XLPEGDA14[b]	110	15	5.8	2.2	5.1

[a] 1 Barrer = 10^{-10} cm^3 (STP) cm/(cm^2 s cm Hg) = 7.5×10^{-18} m^3 (STP) m/(m^2 s Pa).

[b] XLPEGDA values from Kusuma et al. (2008a) and Lin et al. (2005c). Copolymer compositions are reported on a wt% basis.

3.4. Gas transport properties

Crosslinked PEO has been identified as a viable material platform for the production of highly-permeable membranes designed to selectively transport acid gas molecules such as CO_2 over light gases. Amorphous, rubbery PEO networks based on XLPEGDA show favorable transport characteristics when considered within the context of the permeability/selectivity "upper bound" concept (Robeson, 1991), and the introduction of flexible PEG side branches with methyl or ethyl terminal groups has been found to further enhance the permeability of these networks with little or no loss in selectivity (Kusuma et al., 2008b). For the XLBPAEDA networks, transport measurements have been limited to rubbery copolymers synthesized according to the most promising routes for enhanced gas separation performance; i.e., BPAEDA/PEGMEA and BPAEDA/DGEEA. Pure gas permeability measurements were conducted at 35 °C for CO_2, CH_4, H_2, N_2, and O_2, and are reported at infinite dilution. In addition, pure gas solubility measurements were performed at 35 °C for CO_2 and CH_4 (XLBPAEDA homopolymers, only) and are also reported at infinite dilution.

Permeability values for networks based on the BPAEDA4 and BPAEDA15 crosslinkers are presented in Table 3, and selectivity

Table 4
Overall selectivity (P_A/P_B) based on pure gas permeability measured at 35 °C and infinite dilution.

	CO_2/H_2	CO_2/CH_4	CO_2/N_2	O_2/N_2
XLBPAEDA4	2.2	19	55	4.3
85/15 BPAEDA4/PEGMEA	2.8	20	61	4.2
70/30 BPAEDA4/PEGMEA	4.5	17	45	2.7
50/50 BPAEDA4/PEGMEA	6.8	16	44	2.5
25/75 BPAEDA4/PEGMEA	9.7	17	52	2.6
XLBPAEDA15	7.6	18	54	2.6
80/20 BPAEDA15/PEGMEA	8.2	18	57	2.6
70/30 BPAEDA15/PEGMEA	8.4	17	53	2.6
60/40 BPAEDA15/PEGMEA	9.2	17	56	2.6
50/50 BPAEDA15/PEGMEA	9.5	16	51	2.5
80/20 BPAEDA15/DGEEA	7.5	16	49	2.6
70/30 BPAEDA15/DGEEA	7.4	15	43	2.5
60/40 BPAEDA15/DGEEA	7.6	15	43	2.5
50/50 BPAEDA15/DGEEA	7.3	14	46	2.6
XLPEGDA14[a]	7.3	19	50	2.3

[a]XLPEGDA values from Kusuma et al. (2008a) and Lin et al. (2005c).

Table 5
Pure gas solubility and diffusivity at 35 °C and infinite dilution.

	Solubility (cm^3(STP)/cm^3atm)		Diffusivity (cm^2/s)	
	CO_2	CH_4	CO_2	CH_4
XLBPAEDA4	0.940 ± 0.030	0.053 ± 0.027	$(9.62 \pm 0.61)\times10^{-8}$	$(9.0 \pm 4.6)\times10^{-8}$
XLBPAEDA15	1.29 ± 0.03	0.081 ± 0.027	$(8.98 \pm 0.54)\times10^{-7}$	$(7.8 \pm 2.6)\times10^{-7}$
XLPEGDA14[a]	1.30 ± 0.06	0.075 ± 0.028	$(6.18 \pm 0.45)\times10^{-7}$	$(5.5 \pm 2.0)\times10^{-7}$

[a]XLPEGDA values from Kusuma et al. (2008a).

ratios derived from these data are reported in Table 4. Results for the XLPEGDA14 homopolymer network are included for comparison (Kusuma et al., 2008a; Lin et al., 2005c). Solubility data for the XLBPAEDA4 and XLBPAEDA15 networks are reported in Table 5, along with gas diffusivity values calculated according to the solution–diffusion model (i.e., $D = P/S$). The XLBPAEDA15 network shows a CO_2 permeability of 152 Barrer, which is ~40% higher than that obtained with the XLPEGDA14 network. The two homopolymers have similar EO content (80 wt% EO for BPAEDA15 vs. 83 wt% EO for PEGDA14) and display comparable CO_2 and CH_4 solubility, which suggests that a difference in FFV (and corresponding diffusivity) for these materials may be the decisive factor in terms of their relative permeability: XLPEGDA14 has an estimated FFV of 0.120 (Kusuma et al., 2008a), while XLBPAEDA15 has a FFV of 0.125 (see Table 1). The difference in FFV for the two networks is most likely due to the presence of the bulky bisphenol A linkage positioned at the midpoint of the BPA–EDA crosslinker, as well as lower overall crosslink density in the XLBPAEDA15 network. Diffusivity is a strong function of FFV in the XLPEO networks, and the higher permeability and diffusivity values observed for the XLBPAEDA15 network are consistent with the free volume relationships reported previously for the XLPEGDA copolymers; see Kusuma et al. (2008a) and Lin et al., (2006e).

Comparison of the data for the XLBPAEDA4 network relative to XLBPAEDA15 reveals much lower gas permeability values for the XLBPAEDA4 homopolymer. The XLBPAEDA4 network has lower free volume (FFV = 0.118) as compared to XLBPAEDA15 and a much higher effective crosslink density: examination of Table 5 indicates a decrease in the diffusivities of CO_2 and CH_4 by nearly an order of magnitude as compared to XLBPAEDA15. Further, the EO content in XLBPAEDA4 is only about 51 wt%, which is largely responsible for the ~30% decrease in CO_2 solubility observed for the polymer as compared to XLBPAEDA15 or XLPEGDA14. Both factors (i.e., reduced diffusivity and solubility) contribute to the diminished CO_2 permeability measured for the XLBPAEDA4 network.

Interpretation of the selectivity results for the homopolymer networks requires knowledge of the relative size and condensability of the gases; this information is summarized in Lin et al., 2006e. Although both of the BPA–EDA networks under consideration are rubbery at 35 °C, the higher crosslink density and correspondingly lower FFV inherent to the XLBPAEDA4 network renders it more strongly size-sieving in character. As a result, the diffusion of larger penetrants across the membrane is impeded as compared to smaller penetrants. For the XLBPAEDA4 polymer, the combination of lower EO content (i.e., lower CO_2 solubility), as well as greater size sieving, leads to much lower CO_2/H_2 selectivity values as compared to XLBPAEDA15. In cases where CO_2 is the smaller penetrant based on kinetic diameter (e.g., CO_2 (3.3 Å) vs. CH_4 (3.8 Å), or CO_2 vs. N_2 (3.64 Å)), the selectivity values obtained for the XLBPAEDA4 network are nearly the same as those obtained for XLBPAEDA15. In this situation, the reduction in EO content encountered in XLBPAEDA4, which lowers CO_2 solubility, is offset by the additional size discrimination imposed by the membrane, which tends to favor CO_2 diffusion. Thus, even though permeability is reduced for all penetrants, the relative selectivity is preserved. For strictly light gas separations involving smaller O_2 (3.46 Å) vs. larger N_2, size discrimination dominates, leading to markedly higher values of O_2/N_2 selectivity in the XLBPAEDA4 membrane.

The copolymerization of PEG-rich crosslinkers with monofunctional PEG acrylates of varying length and terminal chemistry has been shown to be an effective strategy for the enhancement of gas transport performance in crosslinked PEO membranes. For

the rubbery XLBPAEDA networks, the insertion of flexible ($n = 8$) PEGMEA branches along the network backbone leads to an enhancement in FFV and a corresponding reduction in T_g (*re*: Table 1). Previous studies on XLPEGDA networks suggest that local branch-end defects associated with the methyl-terminated chains are responsible for the observed enhancement in free volume (Borns et al., 2007; Kalakkunnath et al., 2005; Kusuma et al., 2008a; Lin et al., 2006e). In the case of the BPAEDA15 crosslinker, the EO content of the PEGMEA co-monomer (81 wt% EO) and that of the crosslinker are virtually identical, and copolymerization of BPAEDA15 with increasing amounts of PEGMEA does not appreciably alter the overall fraction of EO segments in the resulting network. Accordingly, a significant change in CO_2 solubility in the XLBPAEDA15 polymer would not be anticipated with increasing PEGMEA content (Lin et al., 2006e). The introduction of the PEGMEA branches, however, produces a strong increase in CO_2 transport, with the incorporation of 50 wt% PEGMEA in the pre-polymerization mixture resulting in a doubling of CO_2 permeability. Given the minimal changes in chemical constitution across the copolymer series, the measured increase in permeability can be attributed primarily to an increase in CO_2 diffusivity owing to the observed enhancement in network FFV with increasing branch content.

The permeability of crosslinked PEO based on PEGDA14/PEGMEA has been shown to follow the semi-logarithmic addition model for homogenous copolymers (Lin et al., 2006e; Paul, 1984):

$$\ln P_A = \varphi_1 \ln P_{A,1} + \varphi_2 \ln P_{A,2} \quad (2)$$

where φ_1 and φ_2 are the volume fractions of crosslinker and co-monomer in the polymer, respectively, and $P_{A,1}$ and $P_{A,2}$ are the corresponding permeability coefficients for the 100% crosslinked network and 100% PEGMEA. The volume fractions can be estimated as follows: $\varphi_1 = \rho_P w_1/\rho_1$, where w_1 is the weight fraction of crosslinker in the copolymer, ρ_P is the density of the copolymer, and ρ_1 is the density of the network polymerized from pure crosslinker; $\varphi_2 = 1-\varphi_1$. The model can also be applied to the polymers in this study. CO_2 permeability for the BPAEDA15/PEGMEA copolymer series is plotted vs. crosslinker content in Fig. 11, and compared with the results for PEGDA14/PEGMEA. For both series, the data show good overall correspondence with the addition rule given by Eq. (2), providing a convenient basis for the estimation of copolymer transport performance.

The trends reported for the BPAEDA15/PEGMEA series are in good agreement with analogous studies on crosslinked networks based on bisphenol A ethoxylate dimethacrylate crosslinker ($n = 15$) polymerized with poly(ethylene glycol) methyl ether methacrylate ($n = 9$) co-monomer (Hirayama et al., 1999). The XLBPADMA network encompasses slightly lower overall EO content as compared to XLBPAEDA15, but displays a higher FFV owing to the presence of methyl pendant groups at the crosslink junctions. Copolymerization of the BPADMA15 crosslinker with the methacrylate co-monomer led to a decrease in T_g and a progressive increase in FFV, consistent with the results obtained here. For the methacrylate networks, a CO_2 permeability of 93 Barrer was reported for the homopolymer (25 °C; see experimental details in Hirayama et al., 1999), increasing to 179 Barrer at a ratio of 50/50 wt% crosslinker to co-monomer.

The incorporation of PEGMEA co-monomer into the XLBPAEDA15 network produces rubbery membranes with less size sieving character as compared to the homopolymer. For CO_2/H_2 separations, a lower degree of size discrimination facilitates the permeation of (larger) CO_2 relative to (smaller) H_2, and as a result, the CO_2/H_2 permeability selectivity is observed to increase across the copolymer series. This is an important feature of the crosslinked PEO membranes, as it implies that for this particular separation, the plasticization effect normally associated with the presence of CO_2 can actually improve the separation characteristics (Lin et al., 2006c). A similar

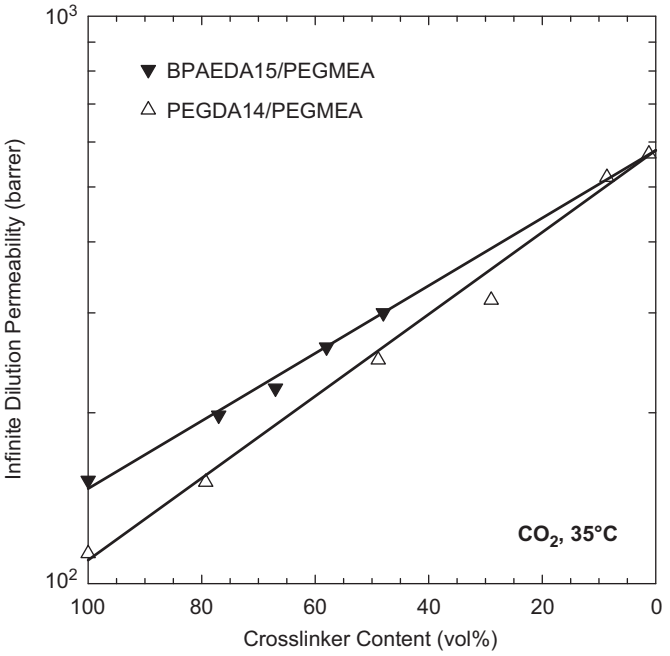

Fig. 11. CO_2 permeability of BPAEDA/PEGMEA copolymer networks; BPA–EDA ($n = 15$) crosslinker. Values for PEGDA14/PEGMEA are plotted as comparison (Lin et al., 2006e). Line is based on the random homogenous copolymer addition model given by Eq. (2).

outcome is observed for the BPAEDA4/PEGMEA series, in which case the measured enhancement in CO_2/H_2 selectivity reflects both an increase in CO_2 affinity for the polymer (owing to a net increase in EO content across the series), as well as reduced size discrimination. It should be noted, however, that the increased FFV associated with the PEGMEA branches leads to a modest reduction in selectivity for binary separations where CO_2 is the smaller of the components (e.g., CO_2/CH_4). Nonetheless, the overall increase in permeability realized by this synthetic strategy would likely outweigh the observed loss of selectivity for many applications.

In a further effort to understand the relationships between network architecture and gas separation performance, the copolymerization of shorter acrylates has been investigated as a means to enhance permeability in crosslinked PEO networks. Prior thermal analysis (Borns et al., 2007) and transport (Kusuma et al., 2008a) studies on XLPEGDA copolymer networks have explored the inclusion of mono-functional acrylates encompassing one or two EO segments, and methyl or ethyl terminal groups. For the BPAEDA15 crosslinker, the inclusion of the ethyl-terminated DGEEA co-monomer was evaluated and its corresponding pure gas transport properties are reported in Tables 3 and 4. The incorporation of DGEEA into the XLBPAEDA15 network involves a trade-off in terms of composition and network architecture. DGEEA encompasses a relatively low EO content (47 wt%) as compared to BPAEDA15, and so the insertion of DGEEA along the network backbone has the potential to reduce CO_2 affinity for the membrane. On the other hand, ethyl-terminated DGEEA appears to be very effective in increasing network free volume, which facilitates permeation for all of the gases. The net result, as detailed in Table 3, is permeability values that are comparable to the BPAEDA15/PEGMEA series when compared on the basis of wt% co-monomer. However, the selectivity values calculated for the BPAEDA15/DGEEA networks are slightly lower than those obtained for the BPAEDA15/PEGMEA copolymers, especially for CO_2/CH_4 and CO_2/N_2 separations wherein CO_2 is the smaller penetrant. For these binary pairs, the enhanced free volume

generated by the DGEEA pendants leads to a lower degree of size discrimination, and this factor, along with a likely reduction in CO_2 affinity, is responsible for the lower CO_2 selectivities encountered with this series.

4. Conclusions

The dynamic relaxation and gas transport properties of homopolymer and copolymer networks based on BPA–EDA crosslinker have been investigated. Three BPA–EDA molecular weights were considered, and dynamic mechanical and dielectric relaxation measurements of the corresponding homopolymer networks reflected both inherent variations in chemical composition and the effective crosslink density encompassed by the monomers. For the highest molecular weight BPA–EDA monomer ($n = 15$), the glass–rubber and sub-glass relaxation characteristics were nearly identical to the properties of XLPEGDA14 model networks studied previously. Copolymerization of the BPA–EDA crosslinkers with flexible PEG monomers was employed as a strategy to control crosslink density and to simultaneously increase the free volume of the membranes. The introduction of methyl- and ethyl-terminated side branches was useful in increasing FFV in the polymers, with the longer PEGMEA segments also producing a significant reduction in glass transition temperature. Transport results for the networks were evaluated within the context of potential trade-offs in CO_2 solubility owing to compositional changes and variations in diffusivity as a result of free volume modifications. The permeability of the XLBPAEDA membranes compared favorably with that reported for XLPEGDA, with the XLBPAEDA15 network displaying CO_2 permeability at infinite dilution that was 40% higher than the value for XLPEGDA14. Here again, the insertion of methyl- or ethyl-terminated PEG branches via copolymerization proved effective in increasing the permeation properties of the membranes, with overall performance approaching or exceeding the literature upper bound for a number of CO_2/light gas pairs.

Acknowledgments

This work was supported in part by a grant from the Kentucky Science and Engineering Foundation as per Grant Agreement KSEF-148-502-05-130 with the Kentucky Science and Technology Corporation. In addition, we are pleased to acknowledge funding from the National Science Foundation Research Experiences for Undergraduates Program administered through the University of Kentucky Center of Membrane Sciences (DMR-0453488). Activities at the University of Texas were supported by the US Department of Energy (Grant DE-FG02-02ER15362) and the US National Science Foundation (Grant CBET-0515425). ^{1}H NMR experiments were performed by Mr. Steven Sorey and Mr. Jim Wallin of the Nuclear Magnetic Resonance Facility, Department of Chemistry and Biochemistry, University of Texas at Austin.

References

Baker, R.W., 2004. Membrane Technology and Applications. second ed. Wiley, New York.

Borns, M.A., Kalakkunnath, S., Kalika, D.S., Kusuma, V.A., Freeman, B.D., 2007. Dynamic relaxation characteristics of crosslinked poly(ethylene oxide) copolymer networks: influence of short chain pendant groups. Polymer 48, 7316–7328.

Colthup, N.B., Daly, L.H., Wiberley, S.E., 1975. Introduction to Infrared and Raman Spectroscopy. Academic Press, New York.

Diaz-Calleja, R., Riande, E., 1997. Calculation of dipole moments and correlation parameters. In: Runt, J.P., Fitzgerald, J.J. (Eds.), Dielectric Spectroscopy of Polymeric Materials. American Chemical Society, Washington, DC, pp. 139–173.

Ferry, J.D., 1980. Viscoelastic Properties of Polymers. third ed. Wiley, New York.

Froehlich, H., 1958. Theory of Dielectrics. Oxford University Press, London.

Gottlieb, H.E., Kotlyar, V., Nudelman, A., 1997. NMR chemical shifts of common laboratory solvents as trace impurities. Journal of Organic Chemistry 62, 7512–7515.

Graham, N.B., 1987. Poly(ethylene oxide) and related hydrogels. In: Peppas, N.A. (Ed.), Hydrogels in Medicine and Pharmacy, vol. II. CRC Press, Boca Raton, pp. 95–113.

Havriliak, S., Negami, S., 1966. Complex plane analysis of α-dispersions in some polymer systems. Journal of Polymer Science, Polymer Symposia 14, 99–103.

Hirayama, Y., Kase, Y., Tanihara, N., Sumiyama, Y., Kusuki, Y., Haraya, K., 1999. Permeation properties to CO_2 and N_2 of poly(ethylene oxide)—containing and crosslinked polymer films. Journal of Membrane Science 160, 87–99.

Jin, X., Zhang, S., Runt, J., 2002. Observation of a fast dielectric relaxation in semicrystalline poly(ethylene oxide). Polymer 43, 6247–6254.

Kalakkunnath, S., Kalika, D.S., Lin, H., Freeman, B.D., 2005. Segmental relaxation characteristics of cross-linked poly(ethylene oxide) copolymer networks. Macromolecules 38, 9679–9687.

Kalakkunnath, S., Kalika, D.S., Lin, H., Freeman, B.D., 2006. Viscoelastic characteristics of UV polymerized poly(ethylene glycol) diacrylate networks with varying extents of crosslinking. Journal of Polymer Science, Part B: Polymer Physics 44, 2058–2070.

Kalakkunnath, S., Kalika, D.S., Lin, H., Raharjo, R.D., Freeman, B.D., 2007a. Molecular dynamics of poly(ethylene glycol) and poly(propylene glycol) copolymer networks by broadband dielectric spectroscopy. Macromolecules 40, 2773–2781.

Kalakkunnath, S., Kalika, D.S., Lin, H., Raharjo, R.D., Freeman, B.D., 2007b. Molecular relaxation in cross-linked poly(ethylene glycol) and poly(propylene glycol) diacrylate networks by dielectric spectroscopy. Polymer 48, 579–589.

Kusuma, V.A., Freeman, B.D., Borns, M.A., Kalika, D.S., 2008a. Influence of chemical structure of short chain pendant groups on gas transport properties of crosslinked poly(ethylene oxide) copolymers. Journal of Membrane Science, in press, doi:10.1016/j.memsci.2008.11.022.

Kusuma, V.A., Lin, H., Freeman, B.D., Jose-Yacaman, M., Kalakkunnath, S., Kalika, D.S., 2008b. Structure/Property characteristics of polar rubbery membranes for carbon dioxide removal. In: Li, N.N., Fane, A.G., Ho, W.S.W., Matsuura, T. (Eds.), Advanced Membrane Technology and Applications. Wiley, New York, pp. 929–953.

Lin, H., Freeman, B.D., 2004. Gas solubility, diffusivity and permeability in poly(ethylene oxide). Journal of Membrane Science 239, 105–117.

Lin, H., Freeman, B.D., 2005a. Materials selection guidelines for membranes that remove CO_2 from gas mixtures. Journal of Molecular Structure 739, 57–74.

Lin, H., Freeman, B.D., 2005b. Gas and vapor solubility in cross-linked poly(ethylene glycol) diacrylate. Macromolecules 38, 8394–8407.

Lin, H., Kai, T., Freeman, B.D., Kalakkunnath, S., Kalika, D.S., 2005c. The effect of crosslinking on gas permeability in cross-linked poly(ethylene glycol) diacrylate. Macromolecules 38, 8381–8393.

Lin, H., Freeman, B.D., 2006a. Gas permeation and diffusion in cross-linked poly(ethylene glycol) diacrylate. Macromolecules 39, 3568–3580.

Lin, H., Freeman, B.D., 2006b. Permeation and diffusion. In: Czichos, H., Saito, T., Smith, L.E. (Eds.), Springer Handbook of Materials Measurement Methods. Springer, Berlin, pp. 371–387.

Lin, H., Van Wagner, E., Freeman, B.D., Toy, L.G., Gupta, R.P., 2006c. Plasticization-enhanced hydrogen purification using polymeric membranes. Science 311, 639–642.

Lin, H., Van Wagner, E., Raharjo, R., Freeman, B.D., Roman, I., 2006d. High-performance polymer membranes for natural-gas sweetening. Advanced Materials 18, 39–44.

Lin, H., Van Wagner, E., Swinnea, J.S., Freeman, B.D., Pas, S.J., Hill, A.J., Kalakkunnath, S., Kalika, D.S., 2006e. Transport and structural characteristics of crosslinked poly(ethylene oxide) rubbers. Journal of Membrane Science 276, 145–161.

Lin, H., Freeman, B.D., Kalakkunnath, S., Kalika, D.S., 2007. Effect of copolymer composition, temperature and carbon dioxide fugacity on pure- and mixed-gas permeability in poly(ethylene glycol)-based materials: free volume interpretation. Journal of Membrane Science 291, 131–139.

Matteucci, S., Yampolskii, Y., Freeman, B.D., Pinnau, I., 2006. Transport of gases and vapors in glassy and rubbery polymers. In: Yampolskii, Y., Pinnau, I., Freeman, B.D. (Eds.), Materials Science of Membranes for Gas and Vapor Separation. Wiley, New York, pp. 1–47.

Paul, D.R., 1984. Gas transport in homogeneous multicomponent polymers. Journal of Membrane Science 18, 75–86.

Priola, A., Gozzelino, G., Ferrero, F., Malucelli, G., 1993. Properties of polymeric films obtained from UV cured poly(ethylene glycol) diacrylates. Polymer 34, 3653–3657.

Robeson, L.M., 1991. Correlation of separation factor versus permeability for polymeric membranes. Journal of Membrane Science 62, 165–185.

Roland, C.M., 1994. Constraints on local segmental motion in poly(vinylethylene) networks. Macromolecules 27, 4242–4247.

Saiz, E., Hummel, J.P., Flory, P.J., Plavsic, M., 1981. Direction of the dipole moment in the ester group. Journal of Physical Chemistry 85, 3211–3215.

Schroeder, M.J., Roland, C.M., 2002. Segmental relaxation in end-linked poly(dimethylsiloxane) networks. Macromolecules 35, 2676–2681.

Treloar, L.R.G., 1975. The Physics of Rubber Elasticity. third ed. Oxford University Press, New York.

Van Krevelen, D.W., 1990. Properties of Polymers: Their Correlation with Chemical Structure, Their Numerical Estimation and Prediction from Additive Group Contributions. Elsevier, Amsterdam.

Williams, G., Watts, D.C., Dev, S.B., North, A.M., 1971. Further considerations of non symmetrical dielectric relaxation behaviour arising from a simple empirical decay function. Transactions of the Faraday Society 67, 1323–1335.